DOI 10.1007/s11204-017-9437-5
Soil Mechanics and Foundation Engineering, Vol. 54, No. 2, May, 2017 (Russian Original No. 2, March-April, 2017)

SOIL MECHANICS

GEOMETRICALLY NONLINEAR BUCKLING STABILITY ANALYSIS OF AXIALLY LOADED UNDERGROUND PIPELINES

UDC 539.3

T. R. Rashidov and E. V. An
Institute of Mechanics and Seismic Stability of Buildings, UAS,
Tashkent, Uzbekistan.

The paper presents an analysis of buckling stability of underground engineering life-support systems, located in water-saturated soils. Analytical and numerical (FEM) solutions are presented and shown to agree well. The influence of soil rheological properties, as well as pipeline geometrical and mechanical parameters on the system dynamic stability, was numerically simulated.

Introduction

Underground engineering life-support systems are used for water, gas, and oil supply, as well as wastewater discharge. Fundamentals of the seismic dynamic theory of orthogonally located underground pipeline systems are described in [1].

The actual construction conditions in seismic areas are complicated by hazardous geological processes (landslides, avalanches, mudflows, collapsible soils, floods, high level of groundwater, etc.). The analysis of underground pipeline stability in water-saturated soils is problematic for all the seismic regions. Papers [2, 3] show that liquefaction of surrounding soils is the main cause for pipeline "surfacing." It is noted in [4] that, in saturated soils, cases of partial pipeline surfacing occurred due to high compressive stresses along the pipeline for all types of underground pipelines [2, 3, 14]. Figure 1 shows typical seismic damages of pipelines.

Pipeline buckling was analyzed by A. S. Volmir, G. Kowderer, D. V. Kapitanov, V. F. Ovchinnikov, L. V. Smirnov, V. I. Maly, H. Uno, F. Oka, S. Tanizaki, A. Tateishi, S. Yasuda, S. Mayuzumi, H. Onose et al. [2, 4-7, 9-12, 14].

Formulation of the problem

Large lateral deformations and a complex stress-strain state of underground pipelines occur as a result of the impact of various operational loads. An underground pipeline can be simulated as a uniform rod, hinged at its ends. A pipeline with length l is divided into finite elements of equal length a with 'nodes' being the ends of these interconnected elements. It is assumed that the nodal displacements are the pipeline generalized coordinates and a compressive force $\vec{P}$ is applied in the cross section $x = 0$ of the first element. According to [5], the same force is acting in any pipeline cross section at any moment in time.

By the Kirchhoff hypothesis [5, 6], the total work of the ith element (with account of its geometric nonlinearity) is

Translated from Osnovaniya, Fundamenty i Mekhanika Gruntov, No. 2, pp. 7-11, March-April, 2017.

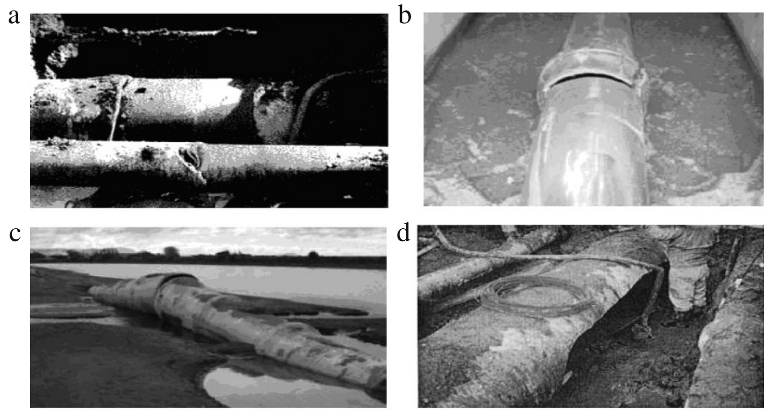

Fig. 1. Pipeline damage types: a) extension/compression cracks; b) pipeline bulging; c) destruction of funnel connections; d) cracks along the pipeline body.

$$A_u^i = \frac{EF}{8}\int_0^a \left(\frac{\partial W_1^i}{\partial x}\right)^4 dx + \frac{EJ}{2}\int_0^a \left(\frac{\partial^2 (W_1^i - W_0^i)}{\partial x^2}\right)^2 dx \tag{1}$$

and the pipeline kinetic energy is

$$E_k^i = \frac{\mu}{2}\int_0^a \left(\frac{\partial W_1^i}{\partial t}\right)^2 dx, \tag{2}$$

where $W_0^i = W_0^i(x)$ and $W_1^i = W_1^i(x, t)$ are initial and total deflection of the ith element; E is the elasticity modulus of the pipe material; J is the axial moment of inertia for the pipe cross section; F is the pipe cross-sectional area; μ is mass per unit length.

The compressive force potential is

$$V_p^i = -\frac{P}{2}\int_0^a \left(\frac{\partial W_1^i}{\partial x}\right)^2 dx. \tag{3}$$

The work of interaction forces between a pipeline element and soil massif is

$$A_{D_1}^i = \frac{1}{2}\int_0^a K(W_1^i - W_0^i)^2 dx;\quad A_{D_2}^i = \frac{1}{2}\int_0^a B\frac{\partial}{\partial t}(W_1^i)^2 dx, \tag{4}$$

where K and B are the coefficients of elastic and viscous pipeline-soil interaction.

The boundary conditions (pipeline is hinged at the ends) are

$$W_1 = 0,\ \frac{\partial^2 W_1}{\partial x^2} = 0 \ \text{ when } \ x = 0,\ l. \tag{5}$$

The shape of the pipeline lateral cross-section is approximated with cubic Hermitian polynomials Θ_1-Θ_4. Denoting the beam deflection in an element located between nodes i and i+1 as $W_1^{i,\,i+1}$ and taking into account the boundary conditions (Eq. (5)), we have

$$W_1^{1,\,2} = \Theta_3 q_3 + \Theta_4 q_4;\ W_1^{2,\,3} = \Theta_1 q_3 + \Theta_2 q_4 + \Theta_3 q_5 + \Theta_4 q_6;\ W_1^{3,\,4} = \Theta_1 q_5 + \Theta_2 q_6 + \Theta_3 q_7 + \Theta_4 q_8;$$

$$W_1^{i,\,i+1} = \Theta_1 q_{2i-1} + \Theta_2 q_{2i} + \Theta_3 q_{2i+1} + \Theta_4 q_{2i+2},\ (i = 2 \ldots n-1);\ W_1^{n,\,n+1} = \Theta_1 q_{2n-1} + \Theta_2 q_{2n},$$

where $Q_1 = 1-\frac{3}{2}\xi^2+\frac{1}{2}\xi^3,\ Q_2 = a\left(\xi-\frac{3}{2}\xi^2+\frac{1}{2}\xi^3\right),\ Q_3 = \frac{3}{2}\xi-\frac{1}{2}\xi^3,\ Q_4 = \left(-\frac{\xi}{2}+\frac{\xi^3}{2}\right),\ \xi = \frac{x}{a};\ q_3,\ q_5,\ q_7\text{-}q_{2i-n}$ are the deflection; q_4, q_6, q_8-q_{2n-1} are the angles of rotation in the nodes [7]; and $q_i = q_i(t)$ are the generalized coordinates.

For a pipeline divided into two elements ($n = 2$), there are three nodes, and $W_1^{1,\,2} = \Theta_3 q_3 + \Theta_4 q_4$, $W_1^{2,\,3} = \Theta_1 q_3 + \Theta_2 q_4$.

The total potential energy Π and the total kinetic energy E_k are as follows:

$$\Pi = \sum_{i=1}^{n} A_u^i + \sum_{i=1}^{n} V_p^i,\quad E_k = \sum_{i=1}^{n} E_k^i. \tag{6}$$

Defining the Lagrange function as $L = E_k - \Pi$, using Eqs. (1)-(4), making some calculations, and inserting the results in the Lagrange equation of the second kind,

$$\frac{d}{dt}\left(\frac{\partial L}{\partial \dot{\bar{q}}_3}\right)-\frac{\partial L}{\partial \bar{q}_3} = -\frac{\partial A_{D1}}{\partial \bar{q}_3}-\frac{\partial A_{D2}}{\partial \dot{\bar{q}}_3};\quad \frac{d}{dt}\left(\frac{\partial L}{\partial \dot{q}_4}\right)-\frac{\partial L}{\partial \bar{q}_4} = -\frac{\partial A_{D1}}{\partial q_4}-\frac{\partial A_{D2}}{\partial \dot{q}_4}, \tag{7}$$

where $L = E_k - A_u - V_p$ and $q_3 = q_3/a$, we obtain

$$\begin{cases} 0.9714\mu a\ddot{\bar{q}}_3+\dfrac{EF}{a^3}[1.44\,\bar{q}_3^3+0.32\,\bar{q}_3 q_4^2]+\dfrac{6EJ}{a^3}(\bar{q}_3-\bar{q}_3^0)-2.4\,\dfrac{P}{a}\,\bar{q}_3 = \\ = -Ka\left(0.9714\ \bar{q}_3-\dfrac{96}{\pi^4}\ \bar{q}_3^0\right)-0.9714Ba\,\dot{\bar{q}}_3; \\ 0.038\mu a\ddot{q}_4+\dfrac{EF}{a^3}[0.32\bar{q}_3^2 q_4+0.04q_4^3]+\dfrac{6EJ}{a^3}q_4-0.4\,\dfrac{P}{a}q_4 = \\ = -0.038Ka\ q_4-0.038Ba\ \dot{q}_4, \end{cases} \tag{8}$$

These equations can be reduced to a system of the first order for the dimensionless variables, $t_1 = t/T_0$, where t_1 and T_0 is a characteristic time constant:

$$\begin{cases} \dfrac{d\bar{q}_3}{dt_1} = y; \\ \dfrac{dy}{dt_1} = \dfrac{-EFT_0^2}{0.9714\mu a^4}\left[1.44\bar{q}_3^3+0.32\bar{q}_3 q_4^2\right]-\dfrac{6EJT_0^2}{0.9714\mu a^4}(\bar{q}_3-\bar{q}_3^0)+\dfrac{2.4PT_0^2}{0.9714\mu a^2}\bar{q}_3- \\ -\dfrac{KT_0^2}{0.9714\mu}\left(0.9714\bar{q}_3-\dfrac{96}{\pi^4}\bar{q}_3^0\right)-\dfrac{BT_0}{\mu}y; \\ \dfrac{dq_4}{dt_1} = z; \\ \dfrac{dz}{dt_1} = \dfrac{-EFT_0^2}{0.038\mu a^4}\left[0.32\bar{q}_3^2 q_4+0.04q_4^3\right]-\dfrac{6EJT_0^2}{0.038\mu a^4}q_4+\dfrac{0.4PT_0^2}{0.038\mu a^2}q_4-\dfrac{KT_0^2}{\mu}q_4-\dfrac{BT_0}{\mu}z. \end{cases} \tag{9}$$

Results and discussion

The developed system of differential equations can be solved by the Runge-Kutta method. Figures 1 and 2 show the curves of maximum amplitudes of underground pipeline lateral motion versus time $t_1 = t/T_0$ when the axial forces are $P(t) = cFt$ and $P = mF_{cr}$, where c is the rate of compression stress variation with time; m is a dimensionless coefficient; and $F_{cr} = 4\pi^2 EJ/l^2$ is the Euler critical force.

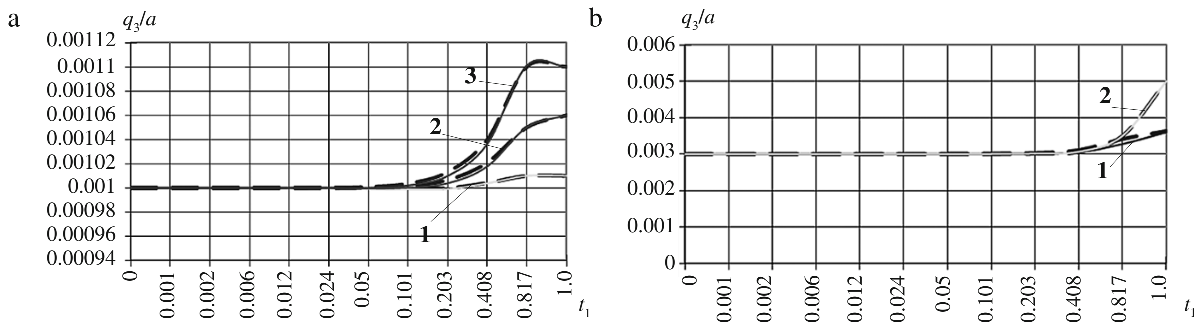

Fig. 2. Maximum amplitude of pipeline lateral motion versus time t_1: ––) analytical; – – –) FEM; a) $c = 10^3$ (1); $c = 5{\cdot}10^3$ (2); $c = 10^4$ (3); b) $T_0 = 0.35$ (1); $T_0 = 0.4$ (2).

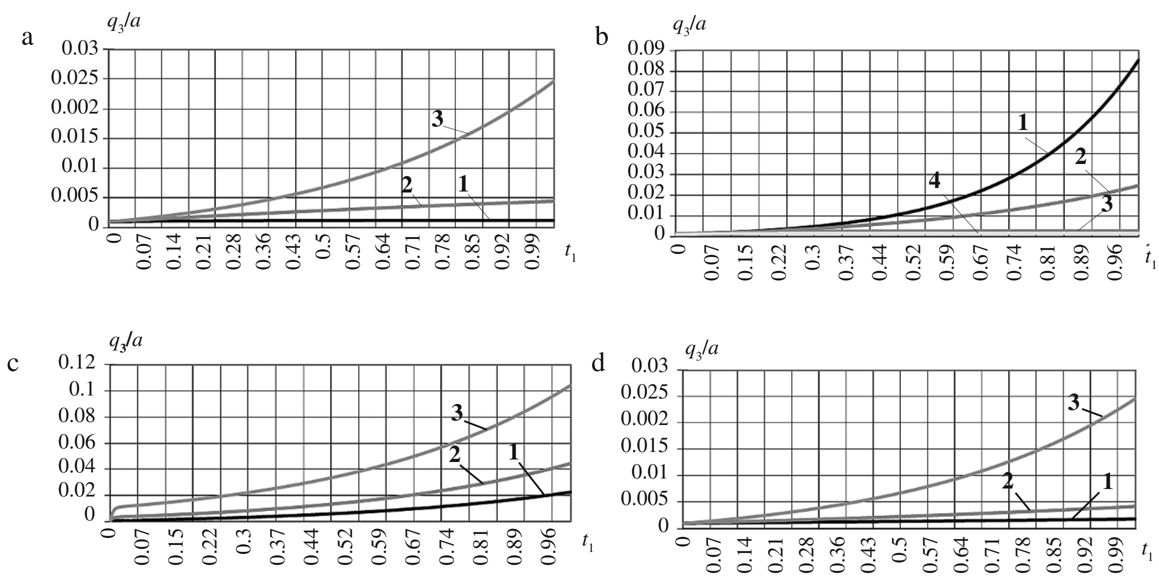

Fig. 3. Lateral movements of underground pipeline versus time at: a) $P = 0.1F_{cr}$ (1); $P = 0.5F_{cr}$ (2); $P = 0.8F_{cr}$ (3); b) $K = 0.5$ (1); 1 (2); 3 (3); 5 (4); c) $y = -0.05$ (1); 0.5 (2); 2 (3); d) $\mu = 1$ (1); 10 (2); 100 (3).

If the pipeline is assumed to be a beam on elastic subgrade, then, assuming $K = k_1 b$ with b as the beam width, k_1 may be regarded as the subgrade stiffness ratio [1]. If we assume that the pipeline is moving laterally in the water-saturated soil with frequency ω, then the coefficient $B = \alpha'(2\sqrt{2}\sqrt{\rho_s \mu_s \omega F})/R$ [8], where α' is the correction coefficient, ρ_s is the soil density, and μ_s is the dynamic viscosity ratio. The calculations were performed for various values of c, T_0, K, B, and the pipeline geometrical parameters. Notably, the analysis of dynamic stability of an underground pipeline was done in [9], where the obtained results were presented as analytical equations, suitable for practical application.

Based on the results of numerical and analytical solutions, we plotted the curves of maximum amplitudes of pipeline lateral motion versus dimensionless time T_0 were plotted (Fig. 2).

Comparison of the curves obtained by numerical method (FEM) and analytically [9] shows that they coincide reasonably well; thus, the possible error is negligible. To evaluate the effect of the other parameters on the pipeline deflection value, the relationships of q_3/a versus time for different values of P, K, μ, and y were calculated (Fig. 3).

Analysis of the obtained curves showed that the greater the longitudinal force, the greater the pipeline deflection. The coefficient K of the elastic pipeline-soil interaction significantly affects the pipeline stability: the greater the coefficient, the greater the pipeline stability. It was found that the greater the action rate, the faster the pipeline reaches dynamic instability with longitudinal load action. The greater the pipeline-soil viscous interaction ratio *B*, the less stable the pipeline. The greater the initial deflection, the greater the pipeline buckling.

By selecting different geometrical parameters of the pipeline, various soil conditions (determined via interaction ratios), and acting loads, it is possible to analyze the peculiarities of the obtained solutions.

At this time, sufficient data on stability of underground life-support systems in soils with different properties have been obtained, e.g., those obtained by Japanese scientists [10], who performed laboratory experiments on a centrifuge to investigate underground pipeline surfacing. The results of our investigations, presented above, coincide well with some of the conclusions in [10]: "The centrifuge dynamic experiments with an underground structure model showed that the rate of pipeline extrusion depends on the initial amplitude and the initial frequency of acceleration, as well as on the stiffness and the attenuation ratio. Soil liquefaction and residual deformations often result in considerable damage of pipeline". [The exact quote was not found.]

Conclusions

Stability analysis of an underground pipeline located in water-saturated soil is one of the most difficult problems of geotechnical engineering. The paper presents and compares analytical and numerical approaches for such analysis.

The validity of the obtained results is supported by concrete examples, showing good coincidence of FEM and the proposed analytical solutions. Additionally, the obtained results coincide well with Russian and worldwide experimental results of earthquake impact on underground pipelines [2, 3, 10, 13, 14] and facilitates further development of the seismic dynamic theory of underground structures.

REFERENCES

1. T. R. Rashidov, *Dynamic Theory of Seismic Stability of Complex Underground Installation Systems* [in Russian], FAN, Tashkent (1973).
2. S. Yasuda, S. Mayuzumi, and H. Onose, "Appropriate countermeasures against liquefaction induced uplift of existing manholes and pipes," *Performance-Based Design in Earthquake Geotechnical Engineering*, 1127-1132 (2009).
3. G. Lanzano, F. Santucci de Magistris, G. Fabbrocino, and E. Salzano, "Multidisciplinary approach for the seismic vulnerability evaluation of lifelines and structural components of industrial plants," *15th World Conference on Earthquake Engineering in Lisbon* (2012).
4. I. Friedmann and B. Debouvry, "Analytical design method helps prevent buried pipe upheaval," *Pipe Line Ind.*, **76**, No. 11, 63-69 (1992).
5. A. S. Volmir, *Stability of Elastic Systems* [in Russian], Nauka, Moscow (1967).
6. G. Kauderer, *Nonlinear Mechanics* [in Russian], IL, Moscow (1961).
7. A. S. Volmir et al, *Problems in Strength of Materials* [in Russian], Nauka, Moscow (1984).
8. L. D. Landau and E.M. Lifshitz, *Fluid Mechanics* [in Russian], Nauka, Moscow (1988).
9. E. V. An and T.R. Rashidov, "Seismodynamics of underground pipelines interacting with water-saturated fine-grained soil," *Mekh. Tverd. Tela*, No. 3, 89-104 (2015).
10. H. Uno, F. Oka, S. Tanizaki, and A. Tateishi, "Centrifuge model tests on the uplift behavior of an underground structure during liquefaction and its numerical modeling," *Performance-Based Design in Earthquake Geotechnical Engineering*, 1127-1132 (2009).
11. V. I. Malyi, "Qualitative analysis of the process of buckling of a rod with a longitudinal impact," *Proc. of International Symposium on Mechanics of Deformable Solids in Honor of A.A. Ilyushin's 95th Birthday Anniversary*, 351-358 (2006).
12. D. V. Kapitanov, V.F. Ovchinnikov, and L.V. Smirnov, "The dynamics of an axially loaded elastic bar after loss of stability," P*robl. Prochn. Plastichn.*, No. 76(3), 205-216 (2014).
13. *The Tashkent Earthquake of 26 April 1966* [in Russian], Akad. Nauk Uzbek. SSR, FAN, Tashkent (1971).
14. K. Yasuko and I. Daisuke, "Liquefaction hotspot based on pipeline damage and topographical history in the Kashima region during the 2011 off the pacific coast of Tohoku earthquake," *15th World Conf. on Earthquake Engineering in Lisbon* (2012).